

# STATUS OF THE EU-XFEL LASER HEATER

M. Hamberg\*, V. Ziemann, Uppsala University, Uppsala, Sweden

## Abstract

We describe the technical layout and the status of the laser heater system for the EuXFEL. The laser heater is needed to increase the momentum spread of the electron beam to prevent micro-bunching instabilities in the linac.

## INTRODUCTION

The electron beam for the EuXFEL [1], is generated in a photo cathode and has such a small momentum spread, that the beam is susceptible to space-charge driven instabilities in the linear accelerator. This problem can be alleviated by increasing the momentum spread of the electron beam in a controlled way. This is done in the laser heater where a laser beam is superimposed to the electron beam that passes through an undulator magnet. If tuned to resonance the transversely oscillating electrons acquire a momentum modulation that is smeared out in a chicane resulting in increased incoherent momentum spread [2-3].

The laser heater consists of several key parts such as the laser system providing the photons, an optical table with optical elements for controlling and shaping the laser beam, a vacuum system for transporting the photons down to the electron interaction point, additional optical tables for control, adjustment and readout of the laser beam, OTR-screens and BPM for overlap adjustments and a compact undulator (see Figure 1).

The laser heater for the XFEL is built up as an in kind contribution from Sweden. We report of the current status and technical layout of the project.

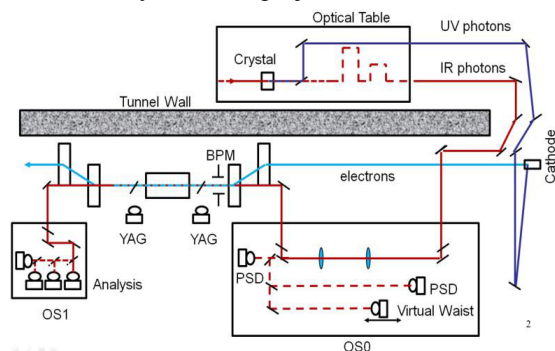


Figure 1: Schematical overview of the laser heater. The IR-laser starts on the optical tables at level 5, continues down a vertical shaft, enter the accelerator tunnel at level 7. The beam is focused, analysed and stabilized on a large optical table before it continues through the interaction region in the undulator and out on a small optical table for analysis.

\*mathias.hamberg@physics.uu.se

## LASER PREPARATION

The laser system is designed and built up at the Max-Born Institute (MBI). The working concept is to use a part of the Nd:YAG laser beam with a wavelength of 1064 nm that is quadrupled in frequency to generate the ultra-violet photons for the photo-cathode electron gun. Deriving the laser-heater photons directly from the gun-laser ensures temporal locking of the electrons and laser throughout the full pulse train of up to 2700, 20 ps pulses with 4.5 MHz repetition rate and the pulsetrains coming at 10 Hz. Moreover the pulse length of laser and electron bunch are matched. Regarding the available pulse energy at XFEL the required output is 50 μJ and a nominal usage of 5 μJ is foreseen.

## ON THE LASER TABLE

Since both laser pulse and electrons stem from the same initial laser oscillator, they have a stable relative temporal relation and we need to provide means to fine adjust the arrival time of the laser pulse in two stages. 1) nano seconds (1-10 ns), static delay line. 2) pico seconds (1-1000 ps), remotely controlled translation stage. These two delay stages are shown as the two bumps on the laser table in the upper right in Fig. 1.

The origin of the arrival time difference is because both laser pulses actually co-propagate for a long way until they reach the accelerator where the UV pulse is propagating upstream towards the laser gun and the IR pulse for the laser heater is propagating downstream to the laser heater chicane. To avoid strong divergence due to diffraction limitation the laser is in an early stage magnified up to ~ 3 mm FWHM.

## LASER TRANSPORT VACUUM SYSTEM

The IR pulses have to be transported from the laser room situated outside the accelerator tunnel (as depicted in Fig. 1) out and down to the optical station 0 (OS0). The total length of the optical beam line will be approximately 50 m and there are 5 mirrors required to guide the laser light to the optical table close to the undulator. Because of the significant distance between the laser room and the undulator, temperature variations can cause convection and fluctuating refractive indices that will disturb the laser beam. It was therefore decided to use an evacuated laser beam pipe.

For the laser transport vacuum system we will use mobile turbo-pump stations to reach initial low pressure that is then maintained by ion pumps. This will reduce the wear on the bearings of the turbo-pumps and will especially limit the vibration level that might disturb the mirrors which are attached to the vacuum beam pipe. Furthermore, thanks to the rather good vacuum, effects

such as dirt buildup on mirrors in moderate vacuum leading to damage can be avoided [4].

At each bend of the laser transport line a special 90-degree corner chamber will be mounted (Fig. 2). These corners are built up with flanges for letting the IR-beam in and out and larger flanges where a mirror mount will be fixed and inspection window can be implemented. The chamber itself is welded to a robust wall-mount. A vacuum test facility for these corners and additional optical components was built up at Uppsala University. Pumping the system showed that the outgassing after 12 days with a mirror mount, actuators and cabling inside was  $3 \times 10^{-5}$  mbar l/s. But continued to go down more quickly compared to a normal metal surface commonly simulated with a  $k/time$  dependence, where  $k$ , is a constant and reached an outgassing rate of about  $7 \times 10^{-7}$  mbar l/s after 39 days (see Fig. 3) [5].

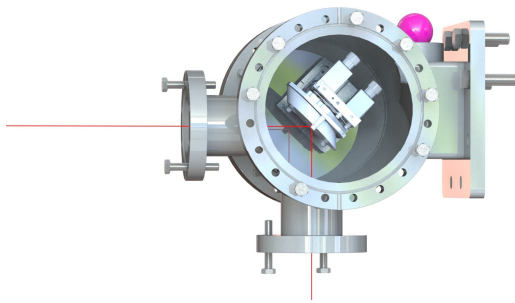


Figure 2: Design of the corner chambers as seen when front DN160 flange is removed. The red line illustrates the laser beam reflecting on the elliptical mirror in the center.

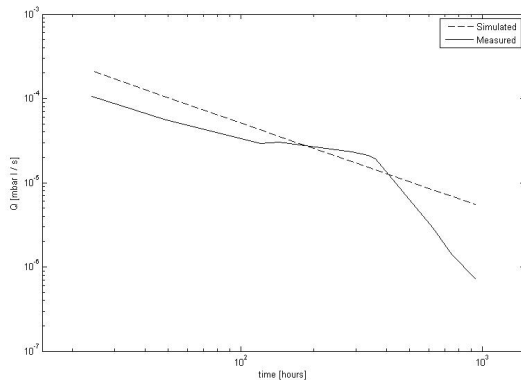


Figure 3: Simulated (dashed line) and measured (solid line) outgassing rate  $Q$  versus time between 24 to 672 hours of pumping.

A vacuum system of such complexity as the entire transport line cannot be built in one fixed block, but sections need to be connected by bellows to permit a small degree of flexibility in particular before and after each corner chamber to decouple the mirror mounts from vibration.

The pressure profile in the laser beam pipe has been simulated with the VAKTRAK program [6]. The laser beam pipe is built up by 3 m long standard sections of

DN63 steel pipes where applicable to ease shipping and assembly and ConFlat (CF) flanges as connectors.

To keep the pressure sufficiently low we will use three 100 l/s pumps between adjacent sections. These will be mounted close to the laser source, just inside of the accelerator tunnel, and close to the end of the vacuum tubing section.

The conductance  $C$  can be estimated from  $C = 11.6 \times d^3/l$ , where  $d$  is the diameter of the round beam pipe in cm and  $l$  is the length in cm.  $C$  is then given in l/s which tacitly assumes that the gas resembles the composition of air at room temperature. To calculate the out-gassing rate we assume that the pipe is made of un-baked steel after 2 weeks of pumping, which has a specific (pessimistic) out-gassing rate of  $K = 4.0 \times 10^{-11}$  torr l/(s cm<sup>2</sup>) and half of that after 4 weeks following a  $1/time$  dependence. The ion pumps are of 100 l/s type, because much stronger ones are of limited use due to the limited conductance. The vacuum corners were simulated as a 60 cm long pipe with the same diameter as the others and using the actually measured outgassing.

The resulting pressure profile is shown in Fig. 4. We see that the minimum pressure after 2 and 4 weeks are about  $2 \times 10^{-7}$  Torr and  $3 \times 10^{-8}$  Torr respectively at the position of the pumps which is acceptable. Gamma Vacuum 100 l/s pumps have a starting pressure of  $< 10^{-3}$  Torr and an estimated lifetime of 50000 hours at  $10^{-6}$  Torr. However, it should be noted that the out-gassing rate will go further down after longer pumping. We also stress that the outgassing measurement of the vacuum corners illustrates a worst case scenario because normal coated cables and anodized mirror mounts were used during tests, which further implies that the outgassing rate should go down significantly with only minor adaptations.

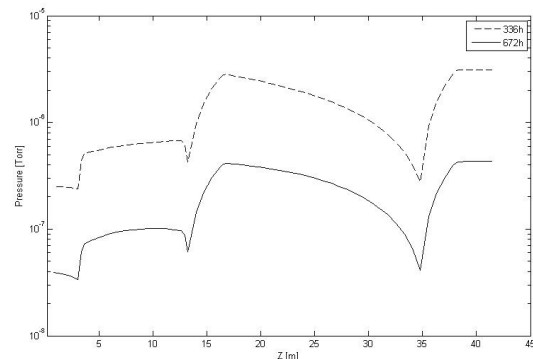


Figure 4: Simulated pressure profile along the laser beam line after 2 (dashed line) and 4 weeks (solid line) of pumping.

## OPTICAL COMPONENTS IN VACUUM

The laser pulse will enter the evacuated beam pipe through a window with an anti-reflex coating. The same type of window will be used near the optical table OS0 (see Fig. 1 and 5) when entering air again. The mirrors to transport the beam from the laser table to OS0 will be

located in vacuum (see Fig. 2). We will use remotely controlled mirror mounts that operate in vacuum and can work with little convective cooling and restricted lubrication. The mirrors will be elliptical with a minimum axis of 2" and mounted in 45 degrees with respect to the incoming beam. The resulting projection will therefore be circular with 2" diameter.

The long evacuated beam pipe might be difficult to align initially. To determine if the mirrors inside vacuum chambers are properly hit by a direct beam we implement photodiodes behind the dielectric mirrors in the corner chambers. Since the dielectric mirrors will leak through  $\sim 0.1\%$  of the light nearly without distorting it, this will permit using a commercially available automated alignment system that center the laser beam on one mirror mount at the time until the beam has reached its target, saving valuable time. This alignment procedure will only be redone if the laser has drifted away significantly from the center of a mirror, this should only happen due to large movements in the building or by accidental impacts on the mirror mount chambers.

## ALIGNMENT STRATEGY AND OPTICAL COMPONENTS AT OS0 AND OS1

There are stringent requirements to match the electron and laser beam with respect to transverse position, size as well as the longitudinal waist position in the undulator [7]. We use a doublet telescope and locate it upstream on the optical table OS0 (see Fig. 1,5) close to the undulator, because that will facilitate to make small laser spots (0.15 mm rms) without excessive beam sizes inside the telescope lenses. The lens mounts must be transversely adjustable so they initially can be aligned to prevent steering when changing their longitudinal position. We will implement adjustable lens mounts on two independently movable slides on a 1.5 m linear translation stage with absolute encoder from SMARACT allowing adjustment of the longitudinal position as well as the width of the waist (see Fig. 5).



Figure 5: Optical station 0 (OS0). The beam enters from top down to the center mirror in the back. It passes the telescope used for beam shaping and the periscope which is used for XY-alignment, and attenuation system before entering the UHV vacuum. Visible are also the two virtual waistlines used for beam stabilization and analysis.

We implement a 'virtual waist' to verify the waist location and spot size. This is achieved by directing a small part of the IR beam immediately after the telescope towards a triggered camera that can move longitudinally in order to scan through the waist (see Fig. 1 and 5). The nominal longitudinal position of the camera must be equal to the position of the center of the undulator. In this way a waist-scan parasitically during operation will give both beam size, waist position and reveal fringe pattern.

Similarly a part of the IR-beam is split out onto the table to two (one for position and one for angle) position sensitive detectors (PSD's) that have sub  $\mu\text{m}$  resolution. They will be implemented as detectors for a 4D stabilization system which will constantly adjust the position and angle of the beam on a pulsetrain to pulsetrain basis. This system utilizes piezo actuators on one mirror close to the laser source and another just before the telescope. In that way a long lever arm is provided. This system will be especially important for long term drifts due to laser pointing, changes in temperature and building deformation. As for the waist-scan, the PSD monitoring the position will be mounted on the optical table at a distance from the telescope corresponding to the center of the undulator (see Fig. 5).

To implement and optimize the performance of the virtual waist camera and 4D-stabilisation system we will need to adjust the attenuation of the IR-laser coupled out from the incoming beam. This is implemented by placing a wheel with dielectric output couplers,  $\lambda/2$  plates and polarizer cubes before the devices to be able to adjust the laser intensity individually. Due to the pulse train range of 1-2700 the dynamic range is large.

Once the beam size and waist position are fixed on the optical bench with the 4D-stabilisation system and investigated by the camera the laser beam position can be adjusted through the undulator. The two last mirrors before entering the UHV electron chamber section are mounted on two translation stages as a periscope and used to steer the XY-position inside the undulator magnet. The angle is adjusted by controlling the tilt of the last mirror.

To verify stable operation a small optical table (OS1, see Fig. 6) is mounted downstream of the undulator. It has an output coupler (beam splitter) mounted such that the major part of the laser light continue to a power meter that constantly monitors the power. The remaining part is attenuated and directed to a camera and PSD to verify that the laser spot position stays unchanged.

For the temporal alignment we will use fast photo diodes on OS1 and a high bandwidth oscilloscope to observe the laser pulse and the spontaneous radiation emitted from the undulator.

The laser operates in the infra-red regime at high power levels and is potentially harmful to humans and equipment (e.g. YAG screen). We therefore need machine protection, interlock systems and also light-tight housing for the optical diagnostic stations.

During commissioning the temporal overlap will be monitored with a transverse deflecting cavity and time

drifts will be measured by a cross-correlation of the laser and the timing system.

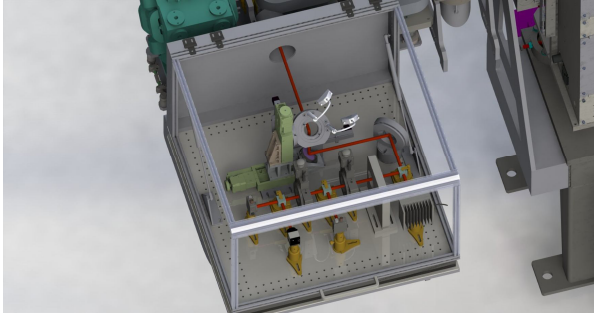


Figure 6: Optical station 1 (OS1). The beam enters from the back of the protection cover to the periscope top. The major part is continuing to a monitoring power meter whereas the rest is attenuated and continues to analysis by PSD, camera and photodiode.

## ELECTRON BEAM VACUUM SYSTEM

The vacuum chambers for the ~2.8 m, UHV linear accelerator section start at the flange upstream of the first dipole and end after the last dipole of the chicane (see Fig. 1). Special attention needs to be paid to the vacuum chambers in dipole 1 and 4 which need view ports to allow the laser pulse to enter and exit the section where it co-propagates with the electron beam in the undulator magnet. To avoid disturbances of the electron beam the magnetic permeability of the chamber material must be kept below  $\mu < 1.01$ , which is demanding to achieve even if using SS 1.4429 (316LN) ESR. The inside of most parts are coated with a  $>2 \mu\text{m}$  copper layer in order to minimize the effect of resistive wall wake fields. Great care are also taken to keep down the inside wall roughness ( $R_{\text{RMS}}$ ) and limiting the oxide layer thickness (O) such that:  $R_{\text{RMS}}(\text{nm}) + 50 \cdot O(\text{nm}) < 1500$  [8].

Detailed analysis of the limited geometries and selected beam parameters was necessary in order to decide whether the last mirror before- and first mirror after the undulator should be mounted inside or outside of vacuum. We decided to place the mirrors inside implying the need of having a metal mirror to avoid charge buildup in dielectric surfaces which would distort the electron beam passing close by ( $\sim 20 \text{ mm}$ ).

The vacuum windows need to be non magnetic which implies that Tantalum attached windows will be used. One beam position monitor (BPM) for timing, steering and energy measurements will be implemented just upstream of the undulator. Adjacent to the undulator there are two movable YAG/CHROMOX-screens with capability to detect both electron beam and laser light. These are used to assure transverse overlap before and after the undulator. The overall design of the UHV chambers can be seen in figure 7.

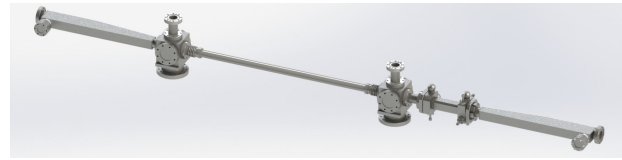


Figure 7: UHV vacuum chamber section. From right to left: Inlet chamber, BPM delivered from DESY, interfacing pipe, OTR-cross, undulator chamber including bellows, OTR-chamber, outlet chamber.

## UNDULATOR MAGNET

The laser and the electron beam interact within the 0.8 m long undulator where the resonant exchange of energy takes place. The magnet, which was ordered and designed by Kyma Technologia, is of Halbach type using NeBFe magnets.

It has 10 periods of 74 mm length of which end periods are special in order to roughly compensate the field integrals. Fine adjustment is done by tuning magnetic fingers which result in a very small variation of the field integrals on the gap setting. The peak field of the undulator of 0.3 T can be reached at a gap setting of 34 mm. The gap is adjusted by servo motors using a Beckhoff PLC controller. Construction was completed in May and mechanical and magnetic field measurements were completed prior to delivery to XFEL in June. We foresee to verify the magnetic measurements on-site later this year. A picture of the undulator prior to shipment is shown in Fig. 8.



Figure 8: Laser heater undulator.

## INTERFACING AND INSTALLATION

The large number of components involved are interfaced to the control system of the XFEL using Beckhoff PLC system which has been shown to be radiation hard and which we have previous experience in configuring and assembly from the ORS project.

Significant cabling work is necessary, especially for fast signal cables for the laser diagnostic diodes, but also to remote-control all components in vacuum. We also provide the mechanical support structure with girder for the undulator and screens. Additionally the OS1, table

need to be removable with the possibility to keep the alignment when remounting it.

## STATUS AND OUTLOOK

We align the schedule such that arrival of most components happens during winter 2013. The UHV vacuum chambers are currently manufactured by FMB Berlin, whereas the undulator is already delivered to DESY by KYMA. Installation of all components occurs during spring 2014. Commissioning follows in two stages: 1) during 2014, commissioning of optical components and system. 2) during 2016, final commissioning investigating the impact of the laser heater on the overall outcome of the XFEL X-rays.

## ACKNOWLEDGEMENTS

It is a pleasure to acknowledge the invaluable help of all DESY groups involved, the high power laser group at Max-Born institute, the UU CAI group, KYMA, FMB Berlin. We thank TEM messtechnik for initial tests and loan of equipment for the 4D stabilization system. We also thank the Swedish research council under project number DNR-828-2008-1093 for financial support.

## REFERENCES

- [1] M. Altarelli, Nucl. Instrum. Methods Phys. Res., Sect. B 269 (2011) 2845.
- [2] Z. Huang et al., Phys. Rev. SPEC. TOP-AC, 13 (2013) 020703.
- [3] S. Spampinati et. al, "COMMISSIONING OF THE FERMI@ELETTRA LASER HEATER" MOPD58, Proceedings of FEL2012, Nara, Japan.
- [4] Y. Cui, H. Yu, Y. Zhao, Y. Jin, H. He and J. Shao, CHIN. OPT. LETT., 5(11) (2007) 680.
- [5] Pfeiffer Vacuum, *Vacuum Technology Know How*, (2012), 22.
- [6] V. Ziemann, "Vacuum tracking", Proceedings of PAC93, Washington DC, USA.
- [7] V.A. Goryashko, V. Ziemann, M. Hamberg and M. Dohlus, "TRANSVERSE ALIGNMENT TOLERANCES FOR THE EUROPEAN XFEL LASER HEATER," THPC097, Proceedings of IPAC2011, San Sebastián, Spain.
- [8] N. Mildner et., Specifications for the Vacuum Sections of the European XFEL, No.:XFEL\_Vacuum 001/2009, Version 2.5 / Dec. 10, (2010); <http://spez.desy.de>